

Available online at www.sciencedirect.com**ScienceDirect**Journal homepage: www.elsevier.com/locate/cortex**Special issue: Research report**

Discriminability of numerosity-evoked fMRI activity patterns in human intra-parietal cortex reflects behavioral numerical acuity

Gabriel Lasne ^{a,b,c}, Manuela Piazza ^{a,b,c,e}, Stanislas Dehaene ^{a,b,c,f},
Andreas Kleinschmidt ^d and Evelyn Eger ^{a,b,c,*}

^a INSERM U992, Gif/Yvette, France

^b CEA, DSV, I2BM, NeuroSpin, Gif/Yvette, France

^c University Paris-Sud, Orsay, France

^d Département of Clinical Neurosciences, University Hospital (HUG) and University of Geneva, Geneva, Switzerland

^e Center for Mind/Brain Sciences, University of Trento, Italy

^f Collège de France, Paris, France

ARTICLE INFO

Article history:

Received 6 November 2017

Reviewed 23 January 2018

Revised 2 March 2018

Accepted 13 March 2018

Published online xxx

Keywords:

fMRI

Parietal cortex

Number processing

Multivariate decoding

Human

ABSTRACT

Areas of the primate intraparietal cortex have been identified as an important substrate of numerical cognition. In human fMRI studies, activity patterns in these and other areas have allowed researchers to read out the numerosity a subject is viewing, but the relation of such decodable information with behavioral numerical proficiency remains unknown.

Here, we estimated the precision of behavioral numerosity discrimination (internal Weber fraction) in twelve adult subjects based on psychophysical testing in a delayed numerosity comparison task outside the scanner. fMRI data were then recorded during a similar task, to obtain the accuracy with which the same sample numerosities could be read out from evoked brain activity patterns, as a measure of the precision of the neuronal representation. Sample numerosities were decodable in both early visual and intra-parietal cortex with approximately equal accuracy on average. In parietal cortex, smaller numerosities were better discriminated than larger numerosities of the same ratio, paralleling smaller behavioral Weber fractions for smaller numerosities. Furthermore, in parietal but not early visual cortex, fMRI decoding performance was correlated with behavioral number discrimination acuity across subjects (subjects with a more precise behavioral Weber fraction measured prior to scanning showed greater discriminability of fMRI activity patterns in intraparietal cortex, and more specifically, the right LIP region).

These results suggest a crucial role for intra-parietal cortex in supporting a numerical representation which is explicitly read out for numerical decisions and behavior.

© 2018 Elsevier Ltd. All rights reserved.

* Corresponding author. INSERM U.992 – Neuroimagerie Cognitive CEA / NeuroSpin, Bâtiment 145, Point Courrier 156, 91191 Gif/Yvette, France.

E-mail address: evelyn.eger@cea.fr (E. Eger).

<https://doi.org/10.1016/j.cortex.2018.03.008>

0010-9452/© 2018 Elsevier Ltd. All rights reserved.

1. Introduction

Humans share with other animals the ability to rapidly extract approximate numerosity from a visual scene, and to compare numerosities with an accuracy that roughly depends on their numerical ratio (Cantlon & Brannon, 2006; Feigenson, Dehaene, & Spelke, 2004). Numerosity perception can be psychophysically dissociated from other quantitative judgments (Anobile, Cicchini, & Burr, 2016; Cicchini, Anobile, & Burr, 2016), suggesting it relies on dedicated neural extraction channels. In accord with this, numerosity responsive units supporting ratio-dependent discrimination can develop through unsupervised learning in hierarchical generative networks (Stoianov & Zorzi, 2012; Zorzi & Testolin, 2017). It is remarkable that the individual precision of basic non-verbal number discrimination can be predictive of current and future higher-level symbolic arithmetic skills (Anobile, Castaldi, Turi, Tinelli, & Burr, 2016; Gilmore, McCarthy, & Spelke, 2007; Halberda, Mazocco, & Feigenson, 2008), even though the human species' particularly highly developed mathematical abilities undoubtedly rely on multiple foundational capacities (Butterworth, 2010; De Smedt, Noel, Gilmore, & Ansari, 2013).

Evidence from several neuroscientific techniques has outlined a set of brain areas with particular importance for numerical processing. In macaque monkeys, single neurons responding differentially to different numbers of perceived items have been described in sub-regions of intra-parietal and prefrontal cortex (Nieder & Miller, 2004; Roitman, Brannon, & Platt, 2007). At a coarse spatial scale, functional MRI has demonstrated increased activation during a variety of numerical as opposed to non-numerical tasks (see Arsalidou & Taylor, 2011, for a meta-analysis), and responsiveness to numerical deviance during passive viewing (e.g., Cantlon & Brannon, 2006; He, Zhou, Zhou, He, & Chen, 2015; Jacob & Nieder, 2009; Piazza, Izard, Pinel, Le Bihan, & Dehaene, 2004), in similarly located regions. In recent years, multivariate decoding methods have been introduced to make fine-grained (e.g., within the same category) discriminations between perceptual features on the basis of fMRI activity profiles across voxels (e.g., Norman, Polyn, Detre, & Haxby, 2006; Tong & Pratte, 2012). Using this approach it has been possible to read out the number seen or held in mind by a subject from fMRI activity in parietal areas functionally equivalent to those carrying numerical responses in macaques (Eger, Pinel, Dehaene, & Kleinschmidt, 2015; Eger et al., 2009). Moreover, beyond pattern-based analyses and the decoding approach, population-receptive field mapping in combination with ultra-high field (7 T) imaging has further allowed recently in humans to detect individual voxels tuned to different numbers of items, in a way very similar to neurons described by macaque neurophysiology (Harvey & Dumoulin, 2017; Harvey, Ferri, & Orban, 2017; Harvey, Klein, Petridou, & Dumoulin, 2013). These tuned responses were found to from orderly topographic layouts in different parietal but also occipital and frontal regions, at least for small non-symbolic numbers.

While the neuronal substrates underpinning numerosity perception have been described in some depth, it remains

insufficiently understood what brain mechanisms give rise to variations in numerical performance, either across subjects or different experimental situations. The ability to read out numerosity information from a given brain area does not necessarily imply that subjects are relying on this information when making numerical discriminations. Recent fMRI studies have shown that numerosity could also be decoded from areas beyond those considered the core substrate of numerical processing, for example early and ventral visual cortex (Bulthé, De Smedt, & Op de Beeck, 2014, 2015; Eger et al., 2015), though not in all cases (Castaldi, Aagten-Murphy, Tosetti, Burr, & Morrone, 2016). Controlling non-numerical properties when working with non-symbolic numerical stimuli is a complex task and often not exhaustively achieved within a single experimental context (Gebuis & Reynvoet, 2012), making positive findings in early visual areas difficult to interpret. Nevertheless, a recent EEG study using an experimental design that allowed testing the effect of variation along multiple non-numerical quantitative dimensions, observed that already very early components of the ERP, compatible with sources in early visual cortex, were modulated more by change in the numerical rather than other dimensions (Park, DeWind, Woldorff, & Brannon, 2016). Such effects could be related to the segmentation of individual items (Dehaene & Changeux, 1993), or the operation of a combination of spatial filters which has been proposed as a potential mechanism to extract an estimate of numerosity (Dakin, Tibber, Greenwood, Kingdom, & Morgan, 2011), plausibly located at earlier levels of the visual hierarchy. Given such potential contributions of earlier visual regions to numerosity extraction, the question arises to what extent numerical acuity as we measure behaviorally is determined by efficiency of the processes at these earlier, or higher-level processing stages as parietal cortex.

To shed light on the question of which, among several areas where numerosity could previously be successfully decoded, are the most critical to determine the precision of behavioral discrimination of this feature, here we related psychophysical measurements and multivariate decoding analysis of fMRI patterns, focusing on variability between subjects and across different numerical ranges. Each subject's precision of behavioral discrimination (internal Weber fraction) was estimated based on psychophysical testing in a delayed numerosity comparison task outside the scanner. fMRI data were then recorded during a similar task, to obtain the accuracy with which the same sample numerosities could be read out from evoked brain activity patterns, as a measure of the precision of the neuronal representation.

2. Materials and methods

2.1. Subjects and MRI acquisition

Twelve healthy volunteers (6 male and 6 female; mean age 22 years) participated in the study. All but one subject were right-handed and all had normal or corrected-to-normal visual acuity. The study was approved by the regional ethical committee (Hôpital de Bicêtre, France).

Functional images were acquired on a 3 T MR system with 12-channel head coil as T2*-weighted echo-planar image (EPI) volumes with 2 mm isotropic voxels. Thirty oblique transverse slices covering essentially the dorsal visual pathway and superior parts of frontal cortex were obtained in ascending interleaved order (repetition time [TR] = 2.52 sec; echo time [TE] = 33 msec; field of view [FOV] = 192 mm; flip angle [FA] = 84°).

2.2. Experimental design and statistical analysis

2.2.1. Stimuli and procedure

During fMRI and in the separate behavioral experiments preceding it, subject performed a delayed numerosity comparison task on displays consisting of different numbers of randomly positioned light gray dots on a black background, inside an implicit circular area subtending ~8° of visual angle at the center of the screen (Fig. 1A). Two separate stimulus sets equated either the overall area of gray (resulting in decreasing dot size with increasing number), or the individual dot size between numerosities (resulting in increasing number of gray pixels with increasing number).

Each trial started with a sample stimulus display for 150 msec, and after a first delay, a match stimulus appeared for 150 msec; after a second delay, a new trial was presented. During the duration of a trial, a red cross was present in the center of the screen, which turned to green for 2 sec after the disappearance of the match stimulus. Subjects had to memorize the approximate number of dots of the sample stimulus on each given trial and to respond by button press, after presentation of the match stimulus, depending on whether they judged the match number smaller or larger than the previous sample number.

Four different sample numerosities separated by a ratio of ~1.6 (8, 13, 21, and 34), were used. For reasons not relevant to the aim of the present report, different ranges of three sample numerosities were presented in different experimental runs (Fig. 1B), the first range comprising numerosities 8, 13, and 21, and the second range numerosities 13, 21 and 34.

In the independent behavioral experiment, six match numerosities were used per sample: (sample 8: 5, 6, 7, 9, 11, and 15 items, sample 13: 8, 9, 11, 15, 18, and 22 items, sample 21: 12, 15, 18, 24, 29, and 36 items, sample 34: 20, 24, 28, 40, 48, and 58 items). Each sample display was separated from the

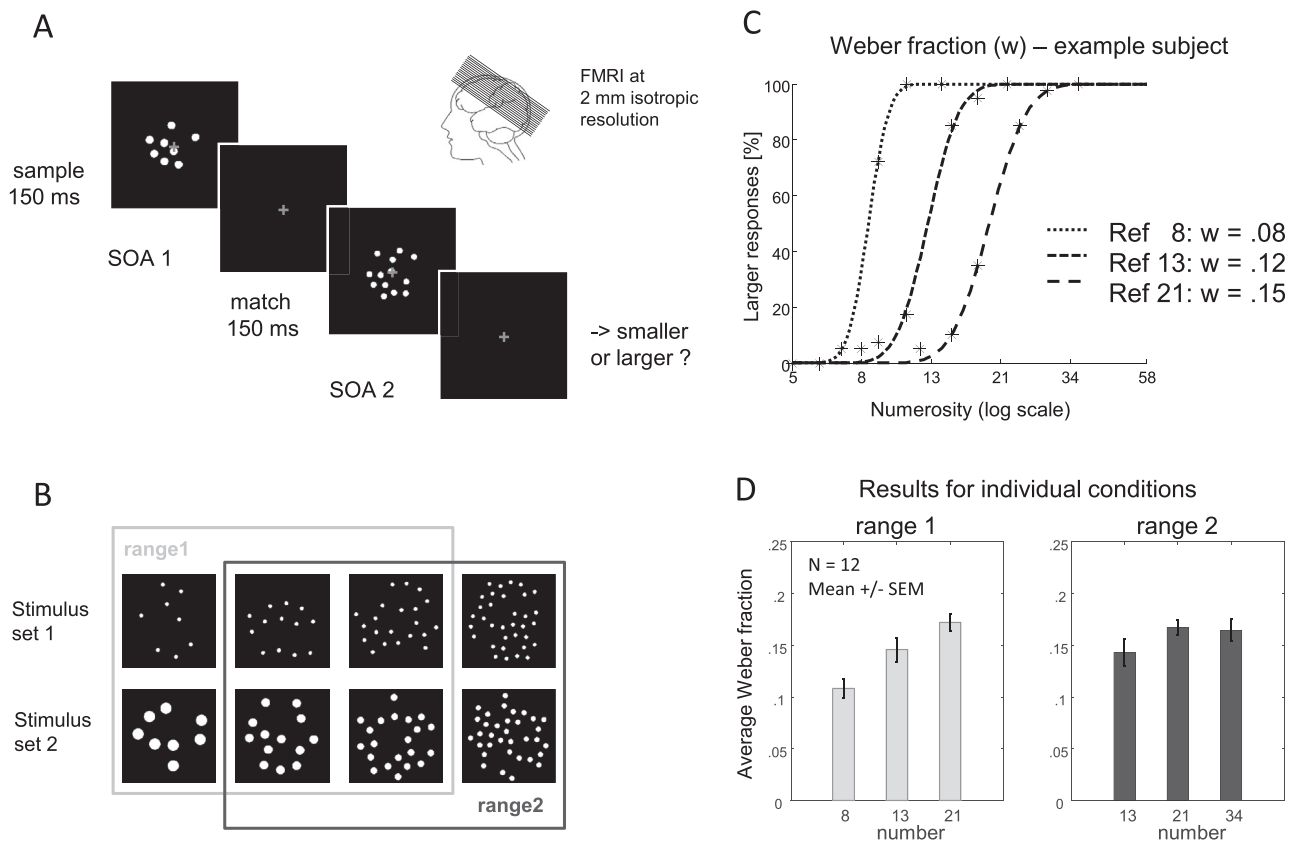


Fig. 1 – Paradigm: A) In a delayed numerical comparison task, subjects were presented with a sample numerosity for 150 msec that after an SOA of several seconds was followed by a match numerosity presented for the same short duration and required a smaller/larger judgment. The critical fMRI data used for multivariate decoding were the responses evoked by the sample numerosities. B) In each half of the experimental runs, three sample numerosities were used, forming two partly overlapping ranges (either 8, 13 and 21, or 13, 21 and 34 items). Behavioral results: The percentage of larger responses in the preceding independent behavioral experiment was fitted with cumulative Gaussian functions to obtain a measure of the internal Weber fraction (w). Panel C) illustrates the functions fitted in one subject, with steeper slopes for smaller numerosities. Panel D) displays group results ($n = 12$, means and SEM) for w obtained for the three sample numerosities in the two ranges.

match display by a stimulus onset asynchrony (SOA 1) of either 3 or 6s, whereas the delay between the match and the new sample presentation (SOA 2) was fixed at 3s. A behavioral run contained 72 trials drawn from the same range of sample numerosities (3 sample numerosities \times 2 SOA 1 \times 6 match numerosities \times 2 set types controlling for different physical variables). Each subject performed a first block of 5 runs with one of the two ranges (e.g., [8–21]), and after a short pause, a second block of 5 runs with the other remaining range (e.g., [13–34]). The order of presentation of these two blocks was counterbalanced across subjects. To obtain a sufficient amount of data, two behavioral testing sessions per subject were performed under the same conditions within an interval of around two weeks.

In the fMRI experiment, to equate subjective task difficulty, match numbers were chosen based on the individual psychometric function of each subject computed from the results of the prior behavioral experiment, using *psignifit* toolbox (<http://psignifit.sourceforge.net/>) (Wichmann & Hill, 2001). Standard match stimuli were chosen to correspond to those numerosities that yielded 25/75% of larger responses in the previous behavioral testing (“standard” trials). In addition, on a small percentage of trials, match numerosities corresponded to 5/95% of larger responses (“catch” trials). The order of trials was pseudo-randomized, as well as the SOA 1 (between sample and match stimulus) and SOA 2 (between match and following sample stimuli), which could be 3, 4, 5 or 6 sec. A run contained 60 “standard” trials (3 samples \times 2 matches \times 2 sets \times 5 repetitions) and 12 “catch” trials (3 samples \times 2 matches \times 2 sets), from the same range of sample numerosities. Each subject performed four runs: run 1 and 4 corresponding to one of the two numerosity ranges, and runs 2 and 3 to the other range, with the order of range presentation counterbalanced across subjects. Before each run, subjects performed a short six-trial-training in which sample and (their respective) match numerosities of the following run were presented. An experiment lasted 45 min.

2.2.2. Data analysis

To obtain measures of the internal Weber fraction of numerosity representation, the percentage of larger responses to match numbers in the psychophysical experiment as a function of the logarithmic difference between sample and match numerosities was fitted with a cumulative Gaussian function, which returned estimates of both the function's standard deviation and mean. The internal Weber fraction is derived from the standard deviation of the fitted Gaussian by dividing it by $\sqrt{2}$ (Dehaene, 2007).

From the Weber fractions for individual numerosities within each range, we further computed the sensitivity index (d') for discrimination between all possible pairs of sample numerosities n_1 and n_2 as in the following way, where w_1 is the internal Weber fraction for n_1 and w_2 the internal Weber fraction for n_2 :

$$d' = \frac{\log(n_1) - \log(n_2)}{\sqrt{w_1^2 + w_2^2}}$$

The fMRI data were preprocessed with SPM8 (<http://www.fil.ion.ucl.ac.uk/spm/software>), including realignment to the first volume as reference, and normalization to the standard

template of the Montreal Neurological Institute (MNI) using SPM's segment algorithm.

The normalized, unsmoothed EPI volumes were entered into a GLM, where each sample stimulus event was modeled as a condition, resulting in 72 conditions per session (60 events for “standard” trials and 12 events for “catch” trials). Match stimulus time points of the same relative magnitude (within the respective range) and response type (smaller or larger than the sample stimulus) were grouped and modeled as further trial types, resulting in 6 additional conditions (3 magnitudes \times 2 response types) per session, intended to capture variance of non-interest related to match stimulus presentation, comparison and response execution.¹ The onsets of these 78 conditions were convolved with a standard hemodynamic response function. The resulting 60 beta estimates (per session) for the “standard” sample stimulus conditions were used in the multi-voxel pattern analysis.

We defined regions of interest (ROIs) by a combination of global masks in MNI space and further subject-specific selection of voxels within each mask. For the analyses of early visual (EV) and parietal cortex (PAR), the global masks were derived from WFU PickAtlas (<http://fmri.wfubmc.edu/software/pickatlas>) (Maldjian, Laurienti, Kraft, & Burdette, 2003) comprising for EV left and right area 17 and for PAR left and right superior and inferior parietal lobules. Within each of these two masks, we selected on a subject-by-subject basis the 600 most significantly activated voxels in the t-contrast of all “standard” sample stimulus conditions versus baseline for decoding analysis. In addition, we targeted more specific sub-regions of parietal cortex, by reapplying the ROIs originally introduced by a previous study (Eger et al., 2015) to operationally define human equivalents of areas LIP and VIP to the current data set. In these cases the global masks corresponded to the group activations of the mentioned previous study thresholded to 300 voxels per ROI and hemisphere as originally done by Eger et al. (2015), and within each of these four masks we selected on a subject-by-subjects basis the 150 most activated voxels in the same contrast (all sample vs baseline) as for the other ROIs.

For pattern classification, conditions were labeled according to sample numerosity, collapsing across the two different stimulus sets. Pattern recognition analysis was performed within each subject on mean-corrected trial-wise parameter estimate vectors (40 vectors/condition) using linear Support Vector Machines (SVM) with regularization parameter $C = 1$ in scikit-learn (<http://scikit-learn.org/stable/>) (Pedregosa et al., 2011). The classification was performed for all possible pairs of numerosities within each range (theoretical chance level = 50%). For each comparison, for trial $n = 1:40$, the n -th trial of each condition was left out for test when training the classifier, and the percentage of correct identification on left-out data was computed across the entire cross-validation cycle.

¹ We verified that sample and match stimulus predictors had a high degree of independence in our design: average cosine similarity between all possible pairs of sample and match stimulus predictors for the same sample numerosity was .048 (for comparison .011 for sample and match stimulus predictors of different sample numerosities, with 0 corresponding to orthogonality and 1 to collinearity).

Confusion matrices were constructed from the output of classifiers from all pairwise comparisons. In addition, in analogy to the analysis of the behavioral data, the sensitivity index (d') was computed for pairwise comparisons between numerosities as:

$$d' = z(\text{hit rate}) - z(\text{false alarm rate})$$

Across subject statistics on behavioral Weber fractions and fMRI classification performance used paired two-tailed t-tests, and the across subject relation between these measures was probed by Pearson correlations.

3. Results

3.1. Behavioral results

We fitted the percentage of larger responses to match numbers with cumulative Gaussian functions to obtain the internal Weber fraction (w) of the numerosity representation (see section 2 for details). Fits were calculated per magnitude, range, sample match delay, and testing session, and subsequently averaged for each magnitude within each range.² Fig. 1C illustrates the fitted curves for one subject, and Fig. 1D the estimated w across subjects for the different conditions. Weber fractions were not completely equal across numerosities in this study, but gradually increased from number 8 to 13 to 21 after which they remained constant. Pairwise statistical comparisons between conditions across the 12 subjects confirmed that Weber fractions for numerosity 8 were significantly different from the ones for all the other conditions (compared to 13 range 1: $t(11) = 3.57, p = .00439$, 21 range 1: $t(11) = 5.71, p = .00014$, 13 range 2: $t(11) = 3.41, p = .00587$, 21 range 2: $t(11) = 7.72, p = .00001$, 34: $t(11) = 3.40, p = .00592$, all paired two-tailed t-tests), while no other comparisons reached significance.

For correlation with the fMRI decoding results, an average Weber fraction across numerosities and ranges was computed for each subject. Across the group these values had a mean of .15 (with the minimum being .13, and the maximum .19).

3.2. fMRI decoding results in early visual and parietal cortex

Multivariate classifiers based on support vector machines were used to discriminate between all pairs of sample numerosities within a given range, within regions of interest

in early visual and parietal cortex. The detailed pattern of classification performance is displayed in Fig. 2A in form of the confusion matrices obtained from the pairwise classification for both regions. Percentages of classification are plotted for the true conditions against the predicted conditions, values on the diagonal reflect correct identifications, and off-diagonal values mis-classifications. Overall accuracies and patterns of performance are rather similar for the two regions of interest, with a slight apparent difference in the accuracy across the two numerical ranges between regions: early visual cortex activation patterns allowed to identify sample numerosities with approximately equal accuracy within both ranges, while in parietal cortex classification was on average better in range 1 which included smaller sample numerosities than in range 2 (as indicated by lower diagonal and higher off-diagonal values). This pattern resembles the one observed in the behavioral results (smaller Weber fractions for smaller numerosities).

Across all pairwise comparisons, decoding performance was on average 57.1% correct in early visual cortex and 56.7% correct in parietal cortex (in both cases significantly different from the theoretical chance level of 50%, paired two-tailed $t(11) = 8.72, p = .000003$ in early visual cortex, and $t(11) = 4.71, p = .000641$ in parietal cortex).

3.3. Across subject correlation between behavioral precision and fMRI decoding performance

To test for the behavioral relevance of these occipital and parietal number representations, we capitalized on the inter-individual differences in the precision of the numerical representation as determined by psychophysics, and correlated the psychophysical Weber fractions across subjects with the average decoding accuracies. The idea underlying this approach is that if a neural representation underpins (or determines) behavior then decoding accuracy should predict psychophysical performance. Fig. 2B shows the extent to which fMRI classification performance is predicted by Weber fractions from the independent behavioral experiment in both regions of interest. In spite of the very similar level of prediction accuracy on average (middle panel), a significant Pearson's correlation of behavioral Weber fractions with fMRI decoding accuracies across subjects was only found in parietal ($r = -.59, p = .0451$) but not early visual cortex ($r = -.07, p = .8305$). A negative correlation in this case indicates that subjects with a higher behavioral acuity (as evidenced by smaller w) have a more precise neuronal representation (as evidenced by higher decoding performance for individual numbers from multi-voxel activation patterns).

The analyses described so far found a relation between decoding performance and behavioral precision in the parietal ROI, which however, was only marginally significant. Furthermore, this correlation appears to depend to a large extent on two subjects with the highest Weber fractions of the group and low (close to chance) decoding performance in the parietal ROI. The two subjects' Weber fractions, however, are still well within the normal range for adult subjects (Piazza et al., 2010), such that they may appear to diverge here only because the rest of the group is rather homogeneous and precise in Weber fraction.

² We also tested in how far Weber fractions differed as a function of the stimulus set (dot size vs total surface area equated between numerosities). In an analysis performing separate fits per stimulus set, magnitude and range, an ANOVA revealed a main effect of stimulus set ($F(1,11) = 17.2, p = .0016$, with average w being .155 for the constant dot size set, and .172 for the constant total surface area set) which, however, did not significantly interact with the other factors. Investigating in detail the influence of stimulus properties on numerical discrimination is beyond the scope of the present study, and for reasons of sensitivity/increasing the number of trials, we subsequently collapsed across the two stimulus sets in both the behavioral and fMRI analyses.

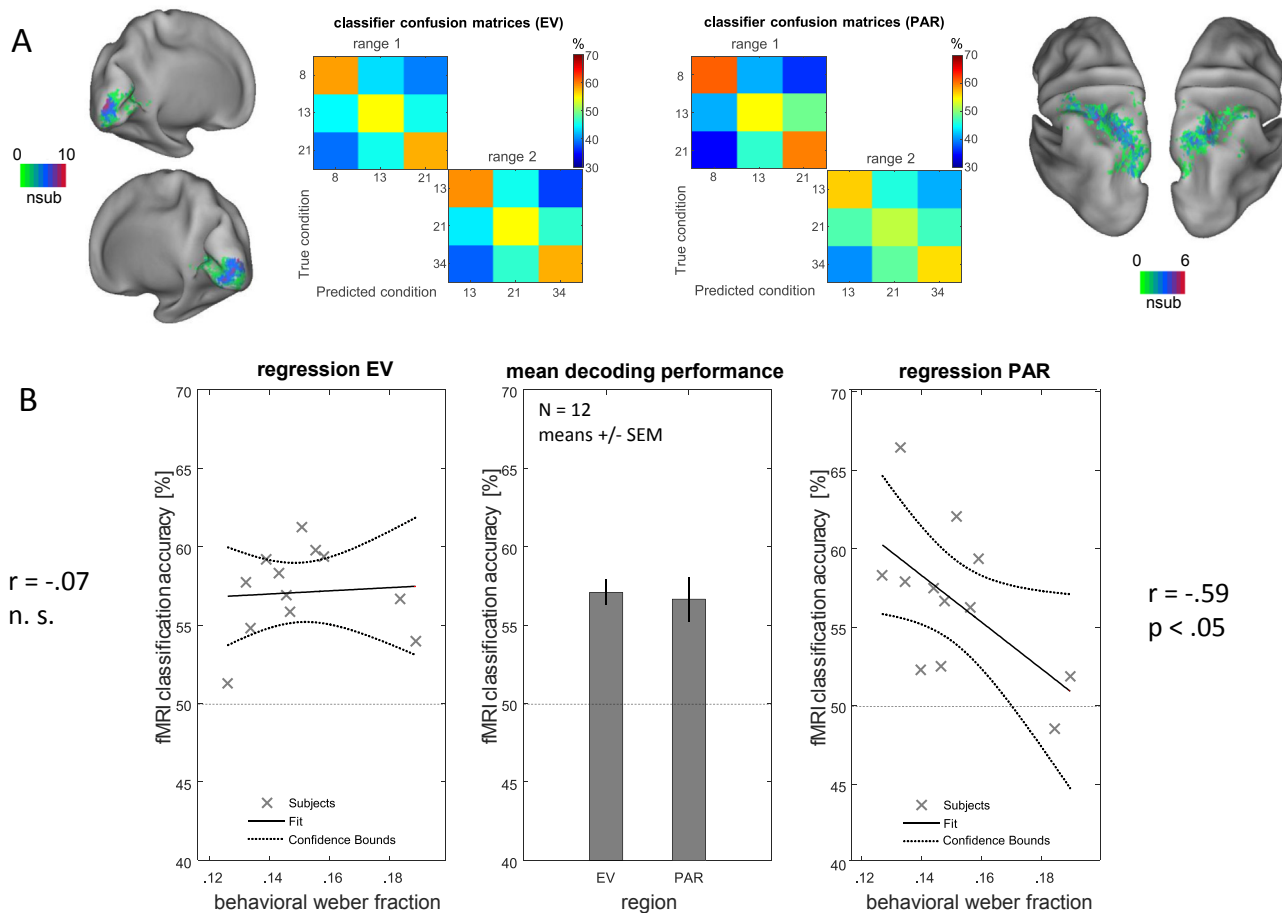


Fig. 2 – fMRI decoding results and across-subject correlation with behavioral Weber fractions in early visual and parietal ROIs: Panel A) displays the ROIs and average confusion matrices obtained from all pairwise classifications between numerosities in each numerical range, for regions of interest in early visual and parietal cortex. Individual subjects' ROIs were defined as the 600 voxels most activated across all sample numerosities vs baseline, within anatomical masks (derived from WFU Pickatlas, see section 2 for details). For the ROI summary displays, rendered onto Caret's PALS Atlas, the color code reflects the number of subjects (out of 12) in whom one given voxel location was included in their specific ROI (smaller values in the parietal cortex reflect a larger variability of the most activated voxels across subjects within the large anatomical mask). In the confusion matrices, the values on the diagonal correspond to the percentage of correct identifications for each numerosity on average across all pairwise comparisons, and the off-diagonal values correspond to the percentages of incorrect identification (confusion with one of the other numerosities). The theoretical chance level for correct identification is 50%. Panel B) displays the average classification performance (means and SEM across the 12 subjects) for pairwise discrimination between numerosities for each ROI (middle panel) together with correlations between individual subjects' fMRI classification performance and behavioral Weber fractions (left panel for early visual cortex, right panel for parietal cortex). In spite of a very similar average decoding performance in the two ROIs, a negative correlation between behavioral w and fMRI decoding performance was found only in the parietal ROI, indicating that subjects with a more precise behavioral discrimination measured prior to scanning had more precisely discriminable evoked activation patterns in that region.

It remains possible that the statistically not very strong results for the parietal ROI are related to the fact that this ROI is rather extended and unspecific in its definition, and not necessarily targeting the most relevant sub-regions/voxels. To further explore the potential contribution of more precise sub-regions of parietal cortex to the observed correlation between behavioral performance and fMRI decoding accuracy, we probed the same relation within four ROIs that were defined in

a previous study using specific functional localizer scans to target the parietal sub-regions which have been implicated in number representations by neurophysiology, representing the putative human equivalents of lateral (LIP) and ventral (VIP) intra-parietal areas of the macaque in the left and right hemispheres (see Fig. 3A for overview of ROI locations). All these regions showed a tendency toward the expected negative correlation, as the one observed in the large and

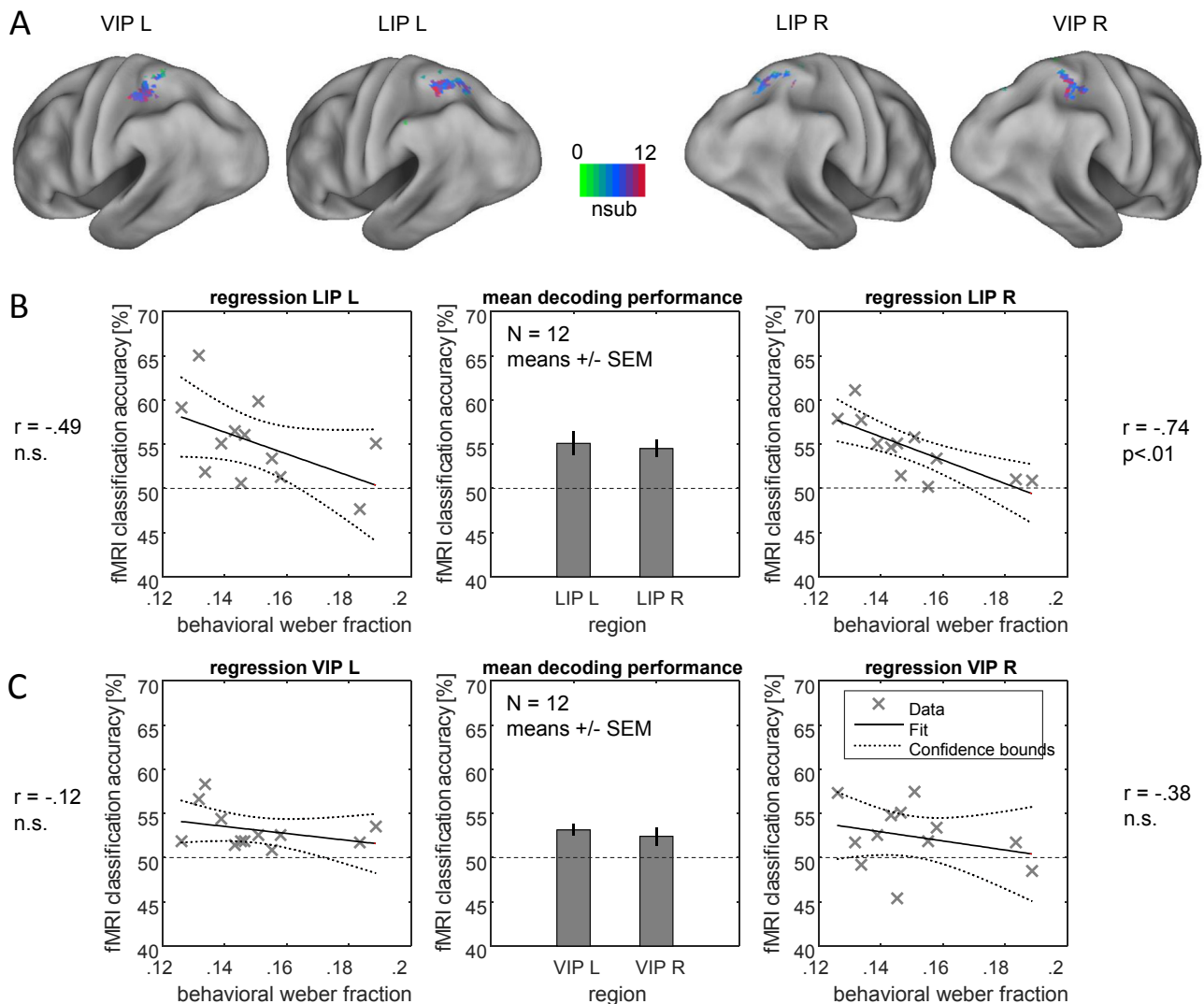


Fig. 3 – FMRI decoding results and across-subject correlation with behavioral Weber fractions in the left and right functional equivalents of areas LIP and VIP: Individual subjects' ROIs were defined as the 150 voxels most activated across all sample numerosities versus baseline, within each of four group-level masks as derived from a previous study (Eger et al., 2015). Panel A) illustrated the ROI locations rendered onto Caret's PALS Atlas, with color codes corresponding, as in Fig. 2, to the number of subjects (out of 12) in whom one given voxel location was included in their specific ROI. Panel B) displays the average classification performance (means and SEM across the 12 subjects) for pairwise discrimination between numerosities (theoretical chance level = 50%) for left and right LIP (middle panel) together with correlations between individual subjects' fMRI classification performance and behavioral Weber fractions (left panel for left hemisphere, right panel for right hemisphere). Panel C) displays the corresponding results for left and right VIP. The negative correlation between behavioral Weber fractions and fMRI decoding performance was only significant in the right LIP ROI when testing all regions in isolation.

unspecific parietal ROI. However, this correlation had the highest value in the right LIP region and it reached significance only in this region when testing each ROI in isolation (right LIP: $r = -.74$, $p = .0059$, left LIP: $r = -.49$, $p = .1067$, right VIP: $r = -.38$, $p = .2266$, left VIP: $r = -.12$, $p = .7053$).³ The correlation in the right LIP region remains significant even when applying

³ The correlation between number decoding and behavioral Weber fractions in the right LIP ROI still remains significant when the two subjects with the largest Weber fractions are taken out ($\rho = -.78$, $p = .0078$).

Bonferroni correction for multiple comparisons in this case (4 subregions tested: $\alpha_{\text{altered}} = .05/4 = .0125$, $p_{\text{corrected}} = .0236$ for right LIP region).

In summary, correlation analyses revealed that subjects with better behavioral discrimination ability between individual numerosities also showed better decodability of numerosity-evoked activity patterns. Critically, this relation was found in parietal cortex, and more specifically in the right LIP region, but not in occipital cortex, even though there was enough information in the latter area to decode numerosity with an equivalent level of performance.

3.4. Behavioral precision and fMRI decoding performance across the numerical range

The results described previously allowed us to establish a relation between individual differences in behavioral numerical acuity and fMRI decoding performance, on average across all the numerosities tested. Behavioral results had also indicated some differences in behavioral precision across the numerical range (in particular smaller Weber fractions for 8 dots than for larger numerosities, see Fig. 1D). In parietal cortex but not in occipital cortex these behavioral results were paralleled by a tendency for better decoding in the range including numerosity 8 (Fig. 2A). To establish a more direct quantitative correspondence between these two tendencies, we computed the sensitivity index (d') for all pairwise discriminations between numerosities from estimated behavioral Weber fractions on the one hand, and the output of the fMRI pattern classifier, on the other hand (see section 2 for details). Fig. 4 displays the resulting d' matrices, for behavioral discrimination (A) and for decoding in early visual and parietal cortex ROIs (B), averaged across subjects. In spite of the fact

that the overall discriminability of fMRI was much lower than the behavioral one, a general pattern of higher d' for comparisons involving the lowest numerosity can be found in the behavioral matrix, and is more clearly reflected in the fMRI decoding matrix from the parietal than the early visual cortex ROI. Multiple regressions on the d' values for the different numerical comparisons, run on a subject-by-subject basis (with predictors being the z-transformed ratio and mean size of the two numerosities in each pair, plus a constant) confirmed that for the behavioral data the beta weights for ratio and size were significantly different from 0 across the 12 subjects (paired two-tailed t-tests: ratio: $t(11) = 23.81, p = 8.2e-11$, size: $t(11) = 3.16, p = 9.1e-03$, Fig. 3C). The same was true for decoding in the parietal cortex ROI (paired two-tailed t-tests: ratio: $t(11) = 4.47, p = .0009$, size: $t(11) = 2.85, p < .0157$), while for the early visual cortex ROI only the ratio predictor reached significance ($t(11) = 5.21, p = .0003$), but the effect of size remained non-significant ($t(11) = .45, p = .6620$) (Fig. 4D).

Thus, decoding performance in parietal cortex closely parallels the observed differences in behavioral discrimination performance across the numerical range, in particular

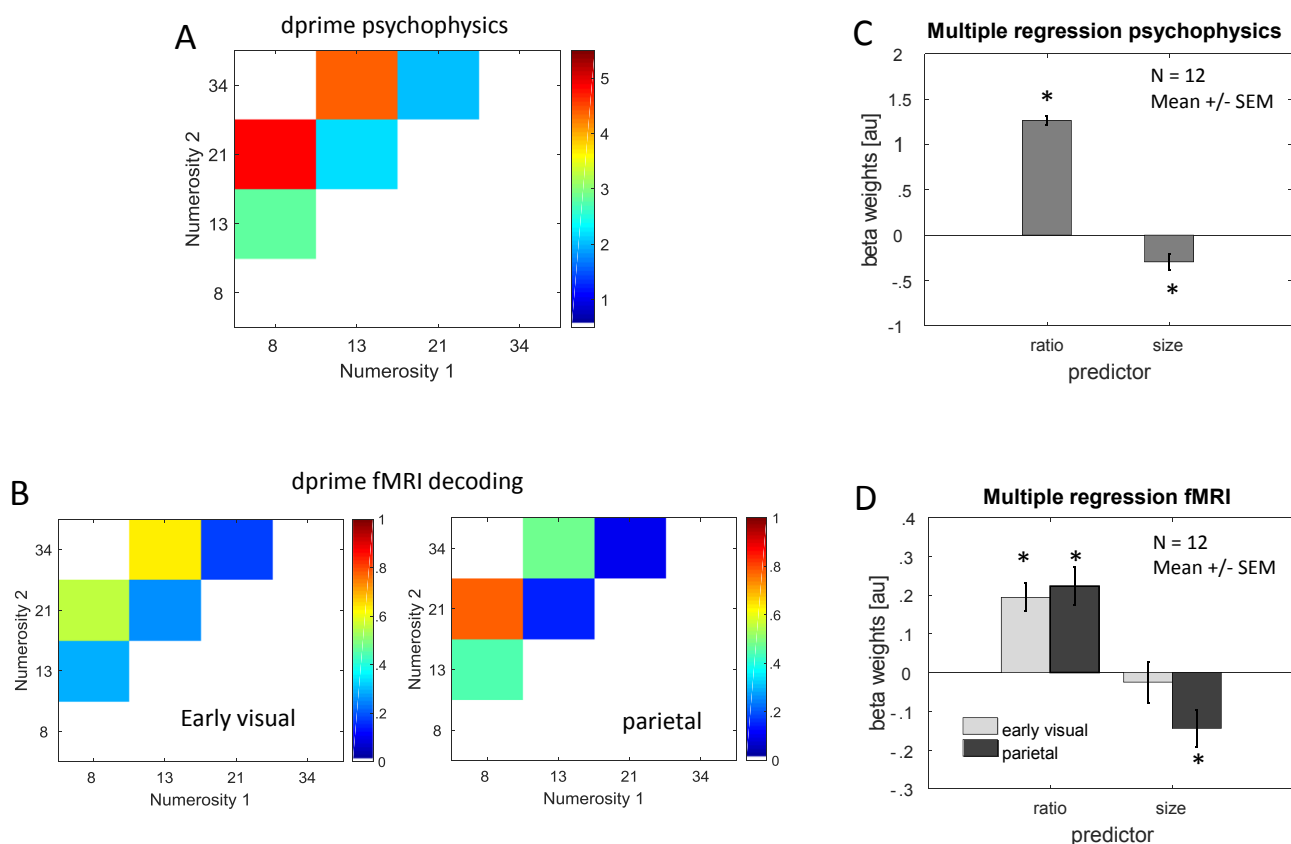


Fig. 4 – fMRI decoding results and behavioral precision across the numerical range: The d' -prime index was calculated for all pairwise comparisons between numerosities (within each of the two numerical ranges) from behavioral Weber fractions and from fMRI decoding performance. Panel A) shows the across subject averages of the d' -prime matrices for behavioral discrimination, and panel B) the ones for fMRI pattern discrimination in early visual and parietal ROIs. A tendency for higher d' -prime values (indicating better discriminability) for comparisons involving smaller as opposed to larger numerosities can be seen in the behavioral results and in the fMRI results from parietal cortex. Multiple regressions, run on a subject-by-subject basis and tested for significance across subjects, confirmed a significant effect of numerical size on top of ratio, for the pairwise discriminability in the behavioral data (C) and the fMRI data of parietal cortex but not early visual cortex (D).

showing a significant effect of the size of two compared numbers on top of their ratio, an effect absent in early visual cortex activity.

4. Discussion

The present study acquired both psychophysical and functional neuroimaging data to test which of several regions previously shown to contain information about individual numerosities is read out when making explicit numerical judgments. We found that in spite of a very similar level of overall decoding performance in early visual and intraparietal cortex, the subjects' behavioral Weber fractions measured prior to scanning were negatively correlated with pattern decoding performance in parietal (and more precisely in the right human equivalent of monkey LIP) but not occipital cortex. This result indicates that the precision with which subjects discriminate numbers reflects the precision with which they represent numbers in specific parietal regions and hence demonstrates that these regions are crucial for overt numerical decisions.

Overall, the fMRI decoding performance reported here (around 57% correct in parietal cortex) may seem low compared to some previous studies (Bulthé et al., 2014; Eger et al., 2009; Knops, Piazza, Sengupta, Eger, & Melcher, 2014). However, when considerably higher decoding performance was obtained previously this was generally for smaller numerosities (up to a maximum of 8 items). When the numerical values and ratios between numerosities were comparable to the ones used here, discrimination performance was considerably lower, and compatible with the one obtained in the current study (Eger et al., 2015). This also fits well with the fact that studies which directly mapped the cortical layout of numerosity selectivity at the level of individual voxels have so far had sufficient sensitivity only to detect preferential responses for relatively small numerosities in parietal cortex (Harvey & Dumoulin, 2017; Harvey et al., 2013).

Given that early visual and parietal cortex allowed us in the present study to decode numerosity to the same degree, one might wonder what might be the nature of the information encoded in early visual cortex. We do not want to claim from the current results that early visual cortex does represent numerosity explicitly (implying individual neurons responsive or tuned to it at that level) and independently from other features. We used in this study two stimulus sets that either equated dot size or the total number of pixels across numerosities. While this is one commonly used strategy for stimulus creation in studies on numerosity perception, it does not control for differences in the total amount and distribution of contrast energy across numerosities, which can affect early visual responses. This factor may likely account for the early visual cortex results in this and other studies, given that the one previous fMRI decoding study which reported successful decoding of numerosity in parietal but not early visual cortex (Castaldi et al., 2016) had equated the contrast energy of the stimuli.

The LIP region defined here by neurophysiologically motivated localizers and showing a strongly significant relation with behavioral acuity is one of the parietal subregions that have been shown in the macaque monkey to contain neuronal

responses discriminating between numerosities (Roitman et al., 2007), with VIP being another one where the majority of neurophysiological recordings were made (Nieder, 2016). Previously we have found that the human equivalents of both regions allowed for decoding of numerosity information for fMRI activity patterns (Eger et al., 2015). The fact that here we did not observe a significant relation of behavioral discrimination with VIP activation patterns does not necessarily mean that no such relation exists. Given the overall reduced decoding performance when the parietal ROI was replaced by several smaller subregions, null results can hardly be considered informative. Nevertheless, in the right LIP a significant relation was found in spite of the reduction in number of voxels, indicating that this region contains the most behaviorally relevant information at least at the spatial scale accessed by our measurements. It is interesting to note a close correspondence between the average MNI coordinates of our right LIP ROI (22.9–61.0 54.2) and the coordinates (23–60 60) where a systematic spatial layout of numerosity responses was observed initially (Harvey et al., 2013) using ultra-high-field fMRI (though without testing the relation of these responses with behavioral numerical acuity).

The present report is the first one showing that the precision of intra-parietal (and more specifically right LIP) activity patterns evoked by individual numerosities reflects inter-individual differences in behavioral numerical acuity in adult human subjects. Interestingly, using fMRI adaptation methods, an across-subject correlation between behavioral Weber fractions and Weber fractions estimated from the fMRI adaptation effect was found very recently in 3–6 year old children (Kersey & Cantlon, 2017) in the right, but not the left intraparietal sulcus. fMRI adaptation and multi-variate decoding of evoked activity patterns are two different approaches often used to tackle similar questions (related to characteristics of neuronal representations), however, the underlying signals exploited by the two methods are of a very different nature. The fMRI adaptation approach is based on deviance signals which are observed at the level of regional activity when a change in the stimulus is introduced (Grill-Spector, Henson, & Martin, 2006), possibly in line with an intrinsic tendency of the brain to predict its input (e.g., Grotheer & Kovács, 2016; Kleinschmidt, Büchel, Hutton, Friston, & Frackowiak, 2002). Multivariate decoding, on the other hand, exploits differences in direct evoked activation patterns, and therefore the layout of responsive neuronal populations, independently from temporal context/stimulation history. Given that such different measures cannot necessarily be guaranteed to provide the same insights, and that they can in fact sometimes lead to different results in the same paradigm and data set (Drucker & Aguirre, 2009), it is even more remarkable that in the case of the relation between perceptual and neuronal sensitivity to numerosity studied here, both measures converge across age groups onto similarly located parietal regions. Beyond this work using fMRI, it is of interest that an across subject correlation has also been observed between the amplitude of ERP components (in particular the N2pc) and numerosity discrimination within the subitizing range, however without allowing to localize the underlying brain regions generating this effect (Ester, Drew, Klee, Vogel, & Awh, 2012).

While as far as we are aware of, inter-individual differences in numerical acuity have not been investigated at the level of single neuron responses, macaque neurophysiology has nevertheless provided evidence for the behavioral relevance of the intraparietal and prefrontal number selectivities: specifically, on trials where the monkeys made errors in a delayed numerosity match-to-sample task, the numerical selectivity for the preceding sample stimulus was lost or reduced (Nieder & Miller, 2004). A related approach using error trials to reveal the relevance of regional activation patterns for performance has also been used in fMRI studies related to other cognitive domains than number: for example, in an experiment on object recognition, on trials when subjects failed to correctly identify the object that was briefly presented and masked, discriminative information was disrupted in lateral occipital object responsive areas, but not in early visual cortex (Williams et al., 2008). Such effects are not necessarily restricted to higher-level cortical areas: decoding of stimulus orientation from early visual cortex was shown to be enhanced on trials where subjects correctly discriminated a small change in orientation as compared to incorrect trials (Scolari & Serences, 2010), and the uncertainty about orientation decoded from early visual cortex on individual trials was found to reflect the variability of perceptual decisions (van Bergen, Ma, Pratte, & Jehee, 2015).

The paradigm we used was less suited to investigate the effects of behavioral relevance at the level of individual trials: subjects were performing a delayed numerosity comparison with two response alternatives (larger or smaller) for which chance performance is 50% and furthermore errors could either arise at the level of encoding of the first or second stimulus, thus minimizing the chances to identify true errors with the amount of trials available in an fMRI experiment as this one. We therefore focused on differences in behavioral precision across subjects and their relation with fMRI decoding. Only one other study to our knowledge has so far reported that decoding performance for a fine-grained perceptual comparison predicted inter-individual differences in behavioral discrimination capacity: in a phoneme discrimination task, decoding of the phonemes/ra and/la differed between English and Japanese speakers, but in addition was also indicative of individual differences in behavioral acuity within groups (Raizada, Tsao, Liu, & Kuhl, 2010). Interestingly, and different from our results, behavioral acuity in that study was related to representations at the earliest stage of cortical processing (Heschl's gyrus).

The across-subject relation with behavioral performance in our case was found for numerosity, but since only numerosity was tested, we cannot claim that the relation is specific for that feature in the regions in question, rather than potentially more generally observed for relevant contents in a comparison task. However, establishing the specificity of the relation between behavior and fMRI decoding for numerosity per se appears a non-trivial enterprise, since successful decoding of numerosity already requires a considerable amount of data/scanning time, and any additional feature to be contrasted with numerosity regarding its correlation with behavioral performance would need to be discriminable within the same regions in the first place.

A related issue is whether the correlation observed necessarily needs to reflect the subjects' intrinsic numerical acuity, rather than variations across subjects in the level of engagement in, or attention to, the task. Attention is well-known to modulate activity in parietal cortex, and pattern recognition methods have revealed that distributed response patterns in intraparietal areas not only can reflect task set (which feature dimension is attended), but also preferentially discriminate between feature values within an attended/task-relevant dimension (e.g., Ester, Sutterer, Serences, & Awh, 2016; Liu, Hospadaruk, Zhu, & Gardner, 2011). Nevertheless, such attentional enhancement of feature information has been found to be at least as present at the earliest stages of the visual hierarchy (e.g., Jehee, Brady, & Tong, 2011; Ling, Pratte, & Tong, 2015; Serences & Boynton, 2007). This contrasts with our study, where we find that only parietal and not early visual cortex patterns reflect behavioral acuity for numerosity across subjects, although our design does not allow us to explicitly rule out effects related to attention in this finding.

In addition to the across subject relation between behavioral acuity and pattern decoding performance for numerosity discrimination, our study also observed differences in numerical acuity across the numerical range tested. Specifically, once again in parietal, but not early visual cortex, smaller numerosities were better discriminated than larger numerosities of the same ratio, paralleling better behavioral precision for the smaller numerosities. Similar findings showing that small numerosities are more discriminable than predicted by Weber's law have been obtained in a few other behavioral studies (Burr, Turi, & Anobile, 2010; Merten & Nieder, 2009). Interestingly, Burr et al. (2010) have shown that the higher behavioral precision for smaller numerosities disappeared when attentional resources were engaged elsewhere, leading to the suggestion that several potential mechanisms contribute to numerosity discrimination across the numerical range, one of which (for relatively small numerosities) requires attentional resources. In our study, the better discriminability of smaller numerosities was not restricted to numbers as small as the ones used in that study and it still remains to be understood in detail which task or stimulus factors determine up to which limit performance for smaller numerosities can deviate from Weber's law.

The findings reported here were obtained during delayed number comparison and thus a working memory task. Further studies will be needed to clarify whether the present correlations between behavioral numerical acuity and the precision of the neuronal representation reflects the precision of the numerical percept per se, or of its maintenance in short-term memory. On the other hand, a previous study has lent support to the idea that the mechanisms for extracting numerosity and non-numerical feature tracking/short term memory of properties of visual sets might be closely intertwined (Knops et al., 2014): Area LIP in particular is thought to implement a saliency map, and a computational model of a saliency map architecture did account for fMRI data acquired with two different tasks in that region by different levels of mutual inhibition between model nodes. It seems tempting to speculate how such a shared component could potentially provide a unifying explanation for diverse impairments found in disorders of numerical processing (dyscalculia) that are

conventionally categorized as either domain-specific (impairments in non-symbolic number processing) or domain-general (impairments in visual working memory) (Piazza et al., 2010; Szucs, Devine, Soltesz, Nobes, & Gabriel, 2013).

To summarize and conclude, the present study is the first one to demonstrate that the precision of numerosity evoked activity patterns in intraparietal cortex, and more specifically the equivalent of area LIP, correlates with behavioral enumeration abilities and thus likely constitutes a crucial level of the cortical hierarchy at which activity is read out for perceptual decisions during numerosity tasks. Future studies may clarify whether this link between behavioral precision and evoked response patterns in intra-parietal cortex is specifically found for numerosity or also for other quantitative or even non-quantitative perceptual contents, what is the role of attention to or task relevance of the feature in question, and what, if any, is the relation between the brain behavior correlation described here and higher-level aspects of numerical performance.

Acknowledgements

This work was funded by the French National Research Agency (ANR). We thank the NeuroSpin platform staff for their assistance in recruiting and scanning volunteers.

REFERENCES

- Anobile, G., Castaldi, E., Turi, M., Tinelli, F., & Burr, D. C. (2016). Numerosity but not texture-density discrimination correlates with math ability in children. *Developmental Psychology*, 52, 1206–1216.
- Anobile, G., Cicchini, G. M., & Burr, D. C. (2016). Number as a primary perceptual attribute: A review. *Perception*, 45, 5–31.
- Arsalidou, M., & Taylor, M. J. (2011). Is $2+2=4$? Meta-analyses of brain areas needed for numbers and calculations. *Neuroimage*, 54, 2382–2393.
- van Bergen, R. S., Ma, W. J., Pratte, M. S., & Jehee, J. F. M. (2015). Sensory uncertainty decoded from visual cortex predicts behavior. *Nature Neuroscience*, 18, 1728–1730.
- Bulthé, J., De Smedt, B., & Op de Beeck, H. P. (2014). Format-dependent representations of symbolic and non-symbolic numbers in the human cortex as revealed by multi-voxel pattern analyses. *Neuroimage*, 87, 311–322.
- Bulthé, J., De Smedt, B., & Op de Beeck, H. P. (2015). Visual number beats abstract numerical magnitude: Format-dependent representation of Arabic digits and dot patterns in the human parietal cortex. *Journal of Cognitive Neuroscience*, 1–12.
- Burr, D. C., Turi, M., & Anobile, G. (2010). Subitizing but not estimation of numerosity requires attentional resources. *Journal of Vision*, 10, 20.
- Butterworth, B. (2010). Foundational numerical capacities and the origins of dyscalculia. *Trends in Cognitive Sciences*, 14, 534–541.
- Cantlon, J. F., & Brannon, E. M. (2006). Shared system for ordering small and large numbers in monkeys and humans. *Psychological Science*, 17(5), 401–406.
- Castaldi, E., Aagten-Murphy, D., Tosetti, M., Burr, D., & Morrone, M. C. (2016). Effects of adaptation on numerosity decoding in the human brain. *Neuroimage*, 143, 364–377.
- Cicchini, G. M., Anobile, G., & Burr, D. C. (2016). Spontaneous perception of numerosity in humans. *Nature Communications*, 7, 12536.
- Dakin, S. C., Tibber, M. S., Greenwood, J. A., Kingdom, F. A. A., & Morgan, M. J. (2011). A common visual metric for approximate number and density. *Proceedings of the National Academy of Sciences of the United States of America*, 108, 19552–19557.
- De Smedt, B., Noel, M.-P., Gilmore, C., & Ansari, D. (2013). How do symbolic and non-symbolic numerical magnitude processing skills relate to individual differences in children's mathematical skills? A review of evidence from brain and behavior. *Trends in Neuroscience and Education*, 2(2), 48–55.
- Dehaene, S. (2007). Symbols and quantities in parietal cortex: Elements of a mathematical theory of number representation and manipulation. In P. Haggard, Y. Rossetti, & M. Kawato (Eds.), *Sensorimotor foundations of higher cognition* (pp. 527–574). Cambridge: Harvard University Press.
- Dehaene, S., & Changeux, J. P. (1993). Development of elementary numerical abilities: A neuronal model. *Journal of Cognitive Neuroscience*, 5, 390–407.
- Drucker, D. M., & Aguirre, G. K. (2009). Different spatial scales of shape similarity representation in lateral and ventral LOC. *Cerebral Cortex*, 19, 2269–2280.
- Eger, E., Michel, V., Thirion, B., Amadon, A., Dehaene, S., & Kleinschmidt, A. (2009). Deciphering cortical number coding from human brain activity patterns. *Current Biology*, 19(19), 1608–1615.
- Eger, E., Pinel, P., Dehaene, S., & Kleinschmidt, A. (2015). Spatially invariant coding of numerical information in functionally defined subregions of human parietal cortex. *Cerebral Cortex*, 25, 1319–1329.
- Ester, E. F., Drew, T., Klee, D., Vogel, E. K., & Awh, E. (2012). Neural measures reveal a fixed item limit in subitizing. *Journal of Neuroscience*, 32, 7169–7177.
- Ester, E. F., Sutterer, D. W., Serences, J. T., & Awh, E. (2016). Feature-selective attentional modulations in human frontoparietal cortex. *Journal of Neuroscience*, 36, 8188–8199.
- Feigenson, L., Dehaene, S., & Spelke, E. (2004). Core systems of number. *Trends in Cognitive Sciences*, 8, 307–314.
- Gebuis, T., & Reynvoet, B. (2012). The interplay between nonsymbolic number and its continuous visual properties. *Journal of Experimental Psychology: General*, 141, 642–648.
- Gilmore, C. K., McCarthy, S. E., & Spelke, E. S. (2007). Symbolic arithmetic knowledge without instruction. *Nature*, 447(7144), 589–591.
- Grill-Spector, K., Henson, R. N., & Martin, A. (2006). Repetition and the brain: Neural model of stimulus-specific effects. *Trends in Cognitive Sciences*, 10, 14–23.
- Grotheer, M., & Kovács, G. (2016). Can predictive coding explain repetition suppression? *Cortex*, 80, 113–124.
- Halberda, J., Mazocco, M., & Feigenson, L. (2008). Individual differences in non-verbal number acuity correlate with maths achievement. *Nature*, 455(7213), 665–668.
- Harvey, B., & Dumoulin, S. (2017). A network of topographic numerosity maps in human association cortex. *Nature Human Behaviour*, 1, s41562–41016-40036-41016.
- Harvey, B., Ferri, S., & Orban, G. (2017). Comparing parietal quantity-processing mechanisms between humans and macaques. *Trends in Cognitive Sciences*, 21, 779–793.
- Harvey, B., Klein, B., Petridou, N., & Dumoulin, S. (2013). Topographic representation of numerosity in the human parietal cortex. *Science*, 341, 1123–1126. <https://doi.org/10.1126/science.1239052>.
- He, L., Zhou, K., Zhou, T., He, S., & Chen, L. (2015). Topology-defined units in numerosity perception. *Proceedings of the National Academy of Sciences of the United States of America*, 112, E5647–E5655.

- Jacob, S. N., & Nieder, A. (2009). Tuning to non-symbolic proportions in the human frontoparietal cortex. *European Journal of Neuroscience*, 30, 1432–1442.
- Jehee, J. F. M., Brady, D. K., & Tong, F. (2011). Attention improves encoding of task-relevant features in the human visual cortex. *Journal of Neuroscience*, 31, 8210–8219.
- Kersey, A. J., & Cantlon, J. F. (2017). Neural tuning to numerosity relates to perceptual tuning in 3- to 6-year-old children. *Journal of Neuroscience*, 37, 512–522.
- Kleinschmidt, A., Büchel, C., Hutton, C., Friston, K. J., & Frackowiak, R. S. J. (2002). The neural structures expressing perceptual hysteresis in visual letter recognition. *Neuron*, 34, 659–666.
- Knops, A., Piazza, M., Sengupta, R., Eger, E., & Melcher, D. (2014). A shared, flexible neural map architecture reflects capacity limits in both visual short-term memory and enumeration. *Journal of Neuroscience*, 34, 9857–9866.
- Ling, S., Pratte, M. S., & Tong, F. (2015). Attention alters orientation processing in the human lateral geniculate nucleus. *Nature Neuroscience*, 18, 496–498.
- Liu, T., Hospadaruk, L., Zhu, D. C., & Gardner, J. L. (2011). Feature-specific attentional priority signals in human cortex. *Journal of Neuroscience*, 31, 4484–4495.
- Maldjian, J. A., Laurienti, P. J., Kraft, R. A., & Burdette, J. H. (2003). An automated method for neuroanatomic and cytoarchitectonic atlas-based interrogation of fMRI data sets. *Neuroimage*, 19, 1233–1239.
- Merten, K., & Nieder, A. (2009). Compressed scaling of abstract numerosity representations in adult humans and monkeys. *Journal of Cognitive Neuroscience*, 21, 333–346.
- Nieder, A. (2016). The neuronal code for number. *Nature Reviews Neuroscience*, 17, 366–382.
- Nieder, A., & Miller, E. K. (2004). A parieto-frontal network for visual numerical information in the monkey. *Proceedings of the National Academy of Sciences of the United States of America*, 101(19), 7457–7462.
- Norman, K. A., Polyn, S. M., Detre, G. J., & Haxby, J. V. (2006). Beyond mind reading: Multi-voxel pattern analysis of fMRI data. *Trends in Cognitive Sciences*, 10, 424–430.
- Park, J., DeWind, N. K., Woldorff, M. G., & Brannon, E. M. (2016). Rapid and direct encoding of numerosity in the visual stream. *Cerebral Cortex*, 26, 748–763.
- Pedregosa, F., Varoquaux, G., Michel, V., Thirion, B., Grisel, O., Blondel, M., et al. (2011). Scikit-learn: Machine learning in Python. *Journal of Machine Learning Research*, 12, 2825–2830.
- Piazza, M., Facoetti, A., Trussardi, A. N., Berteletti, I., Conte, S., Lucangeli, D., et al. (2010). Developmental trajectory of number acuity reveals a severe impairment in developmental dyscalculia. *Cognition*, 116, 33–41.
- Piazza, M., Izard, V., Pinel, P., Le Bihan, D., & Dehaene, S. (2004). Tuning curves for approximate numerosity in the human intraparietal sulcus. *Neuron*, 44, 547–555.
- Raizada, R. D. S., Tsao, F.-M., Liu, H.-M., & Kuhl, P. K. (2010). Quantifying the adequacy of neural representations for a cross-language phonetic discrimination task: Prediction of individual differences. *Cerebral Cortex*, 20, 1–12.
- Roitman, J. D., Brannon, E. M., & Platt, M. L. (2007). Monotonic coding of numerosity in macaque lateral intraparietal area. *PLOS Biology*, 5, 1672–1682.
- Scolari, M., & Serences, J. T. (2010). Basing perceptual decisions on the most informative sensory neurons. *Journal of Neurophysiology*, 104, 2266–2273.
- Serences, J. T., & Boynton, G. M. (2007). Feature-based attentional modulations in the absence of direct visual stimulation. *Neuron*, 55, 301–312.
- Stoianov, I., & Zorzi, M. (2012). Emergence of a 'visual number sense' in hierarchical generative models. *Nature Neuroscience*, 15(2), 194–196.
- Szucs, D., Devine, A., Soltesz, F., Nobes, A., & Gabriel, F. (2013). Developmental dyscalculia is related to visuo-spatial memory and inhibition impairment. *Cortex*, 49, 2674–2688.
- Tong, F., & Pratte, M. S. (2012). Decoding patterns of human brain activity. *Annual Reviews of Psychology*, 63, 483–509.
- Wichmann, F. A., & Hill, N. J. (2001). The psychometric function: I. Fitting, sampling, and goodness of fit. *Perception & Psychophysics*, 63, 1293–1313.
- Williams, M. A., Baker, C. I., Op de Beeck, H. P., Shim, W. M., Dang, S., Triantafyllou, C., et al. (2008). Feedback of visual object information to foveal retinotopic cortex. *Nature Neuroscience*, 11(12), 1439–1445.
- Zorzi, M., & Testolin, A. (2017). An emergentist perspective on the origin of number sense. *Philosophical Transactions of the Royal Society of London. Series B, Biological Sciences*, 373.